Corannulene as a Lewis Base: Computational Modeling of Protonation and Lithium Cation Binding

Maxim V. Frash, Alan C. Hopkinson, and Diethard K. Bohme*

Contribution from the Department of Chemistry, Centre for Research in Mass Spectrometry and Centre for Earth and Space Science, York University, Toronto, Ontario, Canada

Received June 15, 2000

Abstract: A computational modeling of the protonation of corannulene at B3LYP/6-311G(d,p)//B3LYP/6-311G(d,p) and of the binding of lithium cations to corannulene at B3LYP/6-311G(d,p)//B3LYP/6-31G(d,p) has been performed. A proton attaches preferentially to one carbon atom, forming a σ-complex. The isomer protonated at the innermost (hub) carbon has the best total energy. Protonation at the outermost (rim) carbon and at the intermediate (bridgehead rim) carbon is less favorable by ca. 2 and 14 kcal mol^{-1}, respectively. Hydrogen-bridged isomers are transition states between the σ-complexes; the corresponding activation energies vary from 10 to 26 kcal mol^{-1}. With an empirical correction obtained from calculations on benzene, naphthalene, and azulene, the best estimate for the proton affinity of corannulene is 203 kcal mol^{-1}. The lithium cation positions itself preferentially over a ring. There is a small energetic preference for the 6-ring over the 5-ring binding (up to 2 kcal mol^{-1}) and of the convex face over the concave face (3−5 kcal mol^{-1}). The Li-bridged complexes are transition states between the π-face complexes. Movement of the Li^+ cation over either face is facile, and the activation energy does not exceed 6 kcal mol^{-1} on the convex face and 2.2 kcal mol^{-1} on the concave face. In contrast, the transition of Li^+ around the corannulene edge involves a high activation barrier (24 kcal mol^{-1} with respect to the lowest energy π-face complex). An easier concave/convex transformation and vice versa is the bowl-to-bowl inversion with an activation energy of 7−12 kcal mol^{-1}. The computed binding energy of Li^+ to corannulene is 44 kcal mol^{-1}. Calculations of the ^{7}Li NMR chemical shifts and nuclear independent chemical shifts (NICS) have been performed to analyze the aromaticity of the corannulene rings and its changes upon protonation.

1. Introduction

Corannulene (*ghi*,*mno*-dibenzofluoranthene, $C_{20}H_{10}$)[1,2] is an unsaturated hydrocarbon composed of fused rings, one central five-membered and five peripheral six-membered. In the family of polycyclic unsaturated hydrocarbons, corannulene is special in two respects: it is nonplanar, and its carbon skeleton is similar to a surface portion of C_{60} and other fullerenes. Recent studies on corannulene have addressed issues such as efficient preparation,[3−6] the bowl-to-bowl inversion barrier,[4,7−10] ionization energy,[11] electron affinity,[12] and reduction to polyanions by alkali metals.[13,14]

The properties of corannulene as a Lewis base have, to date, received only limited attention. The present work addresses the interaction of corannulene with two quite different types of electrophiles: protons and lithium cations. Taft et al.[15] have compared basicities of a number of organic molecules toward the proton and lithium cation. They have shown that the basicity order for Li^+ may differ markedly from that for H^+, due to hardness/softness and chelation effects. Here we will consider different isomers of protonated and lithiated corannulene; of particular interest are their geometric structures, relative energies, and barriers to transformations between isomers. We also compute the proton and lithium cation affinities of corannulene.

To our knowledge, no measurements of the proton affinity of corannulene have been reported to date. Although some isomers of protonated corannulene have been modeled by electronic structure calculations,[16] the potential energy hypersurface has not been systematically examined. The protonation reactions of some smaller aromatic hydrocarbons have been studied and provide some insight as to what to expect when corannulene is protonated. Thus, benzene accepts a proton forming a σ-complex with a partly destroyed aromatic system.

(1) Barth, W. E.; Lawton, R. G. *J. Am. Chem. Soc.* **1966**, *88*, 380.
(2) Hanson, J. C.; Nordman, C. E. *Acta Crystallogr.*, **1976B**, *32*, 1147.
(3) Scott, L. T.; Hashemi, M. M.; Meyer, D. T.; Warren, H. B. *J. Am. Chem. Soc.* **1991**, *113*, 7082.
(4) Borchardt, A.; Fuchicello, A.; Kilway, K. V.; Baldridge, K. K.; Siegel, J. S. *J. Am. Chem. Soc.* **1992**, *114*, 1921.
(5) Sygula, A.; Rabideau, P. W. *J. Am. Chem. Soc.* **1999**, *121*, 7800.
(6) Seiders, T. J.; Elliot, E. L.; Grube, G. H.; Siegel, J. S. *J. Am. Chem. Soc.* **1999**, *121*, 7804.
(7) Scott, L. T.; Hashemi, M. M.; Bratcher, M. S. *J. Am. Chem. Soc.* **1992**, *114*, 1920.
(8) Sygula, A.; Rabideau, P. W. *THEOCHEM* **1995**, *333*, 215.
(9) Biedermann, P. I.; Pogodin, S.; Agranat, I. *J. Org. Chem.* **1999**, *64*, 3655.
(10) Seiders, T. J.; Baldridge, K. K.; Elliot, E. L.; Grube, G. H.; Siegel, J. S. *J. Am. Chem. Soc.* **1999**, *121*, 739.
(11) Becker, H.; Javahery, G.; Petrie, S.; Cheng, P.-C.; Schwarz, H.; Scott, L. T.; Bohme, D. K. *J. Am. Chem. Soc.* **1993**, *115*, 11636.
(12) Chen, G.; Cooks, R. G.; Corpus, E.; Scott, L. T. *J. Am. Soc. Mass. Spectrom.* **1996**, *7*, 619.
(13) Ayalon, A.; Rabinovitz, M.; Cheng, P.-C.; Scott, L. T. *Angew. Chem., Int. Ed. Engl.* **1992**, *31*, 1636.
(14) Ayalon, A.; Sygula, A.; Cheng, P.-C.; Rabinovitz, M.; Rabideau, P. W.; Scott, L. T. *Science* **1994**, *265*, 1065.
(15) (a) Taft, R. W.; Anvia, F.; Gal, J.-F.; Walsh, S.; Capon, M.; Holmes, M. C.; Hosn, K.; Oloumi, G.; Vasanwala, R.; Yazdani, S. *Pure Appl. Chem.* **1990**, *62*, 17. (b) Burk, P.; Koppel, Ilmar A.; Koppel, Ivar; Kurg, R.; Gal, J.-F.; Maria, P.-C.; Herreros, M.; Notario, R.; Abboud, J.-L. M.; Anvia, F.; Taft, R. W. *J. Phys. Chem. A* **2000**, *104*, 2824.
(16) Maheshwari, S.; Chakraborty, D.; Sathyamurthy, N. *Chem. Phys. Lett.* **1999**, *315*, 181.

10.1021/ja0021464 CCC: $20.00
Published on Web 06/15/2001

High-level electronic structure calculations[17] have established that the σ-complex is the only isomer of protonated benzene at a local minimum; the edge-protonated isomer and π-face complex are at first and second-order saddle points, respectively. Naphthalene can form three distinct protonated σ-complexes whose relative energies can be correlated to aromaticity indices.[18] A good correlation between the computed proton affinities and the measured protodetritiation rates has been found for a number of aromatic hydrocarbons.[18b] Comparisons of the experimental with computed proton affinities of benzene, naphthalene, and azulene will enable us to calibrate our computational scheme.

We did not find reports on the interaction of alkali cations with neutral corannulene. In contrast, complexes of corannulene anions with Li^+ cations have been studied in detail.[13,14] Reduction of corannulene with an excess of lithium metal in THF results in the formation of the sandwich-type complex $(Li^+)_8(C_{20}H_{10}^{4-})_2$, where four Li^+ cations are packed between two corannulene plates, while the remaining four cations are located on the external faces of the two plates.[14] A number of works considered interactions of Li^+ and Na^+ cations with neutral aromatic molecules such as benzene, naphthalene, indole, and pyridine.[19−23] These indicate that the alkali cation preferably coordinates to one of the rings, forming a π-complex. Complexes of metal cations with semi-buckminsterfullerene also have been modeled.[24]

2. Details of the Computations

We had to choose a method of calculations that describes properties of the $C_{20}H_{11}^+$ and $C_{20}H_{10}Li^+$ species with a sufficient accuracy at reasonable computer time expenditure. Previous theoretical studies on corannulene have indicated a good performance of hybrid DFT functionals or MP2 calculations.[9,25,26] Structural parameters of corannulene can be satisfactorally reproduced by these functionals combined with double-ζ plus polarization basis sets,[25,26] while a triple-ζ plus polarization 6-311G(d,p) basis was recommended for the studies of the bowl-to-bowl inversion barrier.[9] Hybrid DFT methods also perform well in the computation of proton affinities.[27]

A hybrid DFT method, B3LYP,[28−30] was employed throughout the present work. In the computations of the protonated corannulene isomers, B3LYP was combined with the 6-311G(d,p) basis set.[31] The performance of the method was checked by comparing the computed and experimental proton affinities of three other cyclic conjugated hydrocarbons: benzene, naphthalene, and azulene (see Section 3.1). Test calculations on the proton affinity of benzene (see Supporting Information) indicated that an increase of the basis set size beyond 6-311G(d,p) or use of different DFT methods instead of B3LYP does not alter the results significantly.

For the interaction of corannulene with Li^+ cations, we used a slightly different strategy than for protonation. Geometries of the species involved were optimized at B3LYP/6-31G(d,p),[28−30,32] and then single-point calculations were performed at B3LYP/6-311G(d,p). A check with the parent corannulene and three selected structures (π_5, π_{5i}, and TS for bowl-to-bowl inversion π_5 to π_{5i}, in Table 5) indicated that this procedure yields results very close to the B3LYP/6-311G(d,p) optimization (r_{C-C} and r_{C-H} are within 0.004 Å, r_{C-Li} within 0.013 Å, Li^+ coordination energies and the bowl-to-bowl inversion barrier within 0.2 kcal mol^{-1}). BSSE corrections[33] were computed using a formula that distinguishes between the basis set and geometry change effects,[34] and were included in the computed electronic energies. The procedure was tested by computing the interaction energy of Li^+ with benzene and the result (−37.4 kcal mol^{-1}) is close to the values obtained from experiment (−37.0 kcal mol^{-1})[35] and high-level computations (G2:[36] −36.7 kcal mol^{-1}; CBS-QB3:[37] −35.4 kcal mol^{-1}). An increase of the basis set size beyond 6-311G(d,p) does not alter the result significantly (see Supporting Information).

The calculations were carried out with the Gaussian 98 program.[38] The natural charges[39] were computed using the NBO program[40] incorporated in Gaussian 98. The nature of the obtained stationary points was analyzed by analytical frequency calculations. The reactants and products interconnected by each transition state were verified with the IRC method,[41] unless otherwise stated in the text. The reaction enthalpies at 298 K were computed from the electronic energies by adding zero-point energies, the PV work terms, and thermal contributions.

The NMR shielding constants have been computed using the GIAO method[42] (implemented[43] in Gaussian 98) at the MPW1PW91/6-311G(d,p) level, using geometries optimized at B3LYP/6-311G(d,p) (corannulene and protonated corannulene isomers) or B3LYP/6-31G(d,p) (corannulene and its complexes with Li^+). Wiberg has shown[44] that the MPW1PW91[45,46] functional reproduces very well the experimental shielding constants and is superior to B3LYP for that purpose. The ^{13}C shielding constant in tetramethylsilane (TMS, the usual reference compound in ^{13}C NMR measurements) computed with the method chosen is 188.8 ppm, which is very close to the experimental value of

(17) Glukhovtsev, M. N.; Pross, A.; Nicolaides, A.; Radom, L. *J. Chem. Soc., Chem. Commun.* **1995**, 2347.
(18) (a) Kovacek, D.; Maksic, Z. B.; Novak, I. *J. Phys. Chem. A* **1997**, *101*, 1147. (b) Streitwieser, A.; Wang, D. Z. *Theor. Chem. Acc.* **1999**, *102*, 78.
(19) Dunbar, R. C. *J. Phys. Chem. A* **1998**, *102*, 8946.
(20) Hashimoto S.; Ikuta, S. *THEOCHEM* **1999**, *468*, 85.
(21) Cubero, E.; Orozco, M.; Luque, F. J. *J. Phys. Chem. A* **1999**, *103*, 315.
(22) Nicholas, J. B.; Hay, B. P.; Dixon, D. A.*J. Phys. Chem. A* **1999**, *103*, 1394.
(23) Hoyau, S.; Norrman, K.; McMahon, T. B.; Ohanessian, G. *J. Am. Chem. Soc.* **1999**, *121*, 8864.
(24) Sygula, A.; Rabideau, P. W. *J. Chem. Soc., Chem. Commun.* **1994**, 2271.
(25) Martin, J. M. L. *Chem. Phys. Lett.* **1996**, *262*, 97.
(26) Baldridge, K. K.; Siegel, J. S. *Theor. Chem. Acc.* **1997**, *97*, 67.
(27) Jursic, B. S. *THEOCHEM* **1999**, *487*, 193.
(28) Stephens, P. J.; Devlin, F. J.; Chabalowski, C. F.; Frisch, M. J. *J. Phys. Chem.* **1994**, *98*, 1623.
(29) (a) Becke, A. D. *J. Chem. Phys.* **1993**, *98*, 1372. (b) Becke, A. D. *J. Chem. Phys.* **1993**, *98*, 5648.
(30) Lee, C.; Yang, W.; Parr, R. G. *Phys. Rev. B* **1988**, *37*, 785.
(31) Krishnan, R.; Binkley, J. S.; Seeger, R.; Pople, J. A. *J. Chem. Phys.* **1980**, *72*, 650.
(32) (a) Ditchfield, R.; Hehre, W. J.; Pople, J. A. *J. Chem. Phys.* **1971**, *54*, 724. (b) Hehre, W. J.; Ditchfield, R.; Pople, J. A. *J. Chem. Phys.* **1972**, *56*, 2257. (c) Hariharan, P. C.; Pople, J. A. *Theor. Chim. Acta* **1973**, *28*, 213. (d) Dill, J. D.; Pople, J. A. *J. Chem. Phys.* **1975**, *62*, 2921.
(33) Boys, S. F.; Bernardi, F. *Mol. Phys.* **1970**, *19*, 553.
(34) Bates, S.; Dwyer, J. *J. Phys. Chem.* **1993**, *97*, 5897.
(35) Staley, R. H.; Beauchamp, J. L. *J. Am. Chem. Soc.* **1975**, *97*, 5920.
(36) Curtiss, L. A.; Raghavachari, K.; Trucks, G. W.; Pople, J. A. *J. Chem. Phys.* **1991**, *94*, 7221.
(37) Montgomery, J. A., Jr.; Frisch, M. J.; Ochterski, J. W.; Petersson, G. A. *J. Chem. Phys.* **1999**, *110*, 2822.
(38) Frisch, M. J.; Trucks, G. W.; Schlegel, H. B.; Scuseria, G. E.; B. G.; Robb, M. A.; Cheeseman, J. R.; Zakrzewski, V. G.; Montgomery, J. A.; Stratmann, R. E.; Burant, J. C.; Dapprich, S.; Millam, J. M.; Daniels, A. D.; Kudin, K. N.; Strain, M. C.; Farkas, O.; Tomasi, J.; Barone, V.; Cossi, M.; Cammi, R.; Mennucci, B.; Pomelli, C.; Adamo, C.; Clifford, S.; Ochterski, J.; Petersson, A.; Ayala, P. Y.; Cui, Q.; Morokuma, K.; Malick, D. K.; Rabuck, A. D.; Raghavachari, K.; Foresman, J. B.; Cioslowski, J.; Ortiz, J. V.; Stefanov, B. B.; Liu, G.; Liashenko, A.; Piskorz, P.; Komaromi, I.; Gomperts, R.; Martin, R. L.; Fox, D. J.; Keith, T.; Al-Laham, M. A.; Peng, C. Y.; Nanayakkara, A.; Gonzalez, C.; Challacombe, M.; Gill, P. M. W.; Johnson, B. G.; Chen., W.; Wong, M. W.; Andres, J. L.; Head-Gordon, M.; Replogle, E. S.; Pople, J. A. *Gaussian 98*, Revision A.5; Gaussian, Inc.: Pittsburgh, PA, 1998.
(39) Reed, A. E.; Curtiss, L. A.; Weinhold, F. *Chem. Rev.* **1988**, *88*, 899.
(40) Glendening, E. D.; Reed, A. E.; Carpenter, J. E.; Weinhold, F. *NBO* Version 3.1.
(41) (a) Gonzalez, C.; Schlegel, H. B. *J. Chem. Phys.* **1989**, *90*, 2154. (b) Gonzalez, C.; Schlegel, H. B. *J. Phys. Chem.* **1990**, *94*, 5523.
(42) Ditchfield, R. *Mol. Phys.* **1974**, *27*, 789.
(43) Cheeseman, J. R.; Trucks, Gary W.; Keith, T. A.; Frisch, M. J. *J. Chem. Phys.* **1996**, *104*, 5497.
(44) Wiberg, K. B. *J. Comput. Chem.* **1999**, *20*, 1299.
(45) Adamo, C.; Barrone, V. *Chem. Phys. Lett.* **1997**, *274*, 242.
(46) Perdew, J. P.; Burke, K.; Wang, Y. *Phys. Rev.* **1996**, *B54*, 16533.

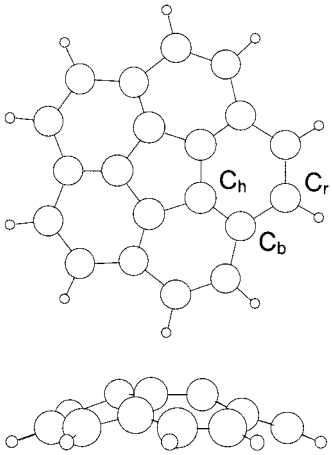

Figure 1. The structure of corannulene. Large open circles, carbons; small open circles, hydrogens. Carbon atom types: C_h, hub; C_r, rim; and C_b, bridgehead rim.

186.4 ppm.[47] Use of the larger 6-311G(2d,p) or 6-311+G(d,p) basis sets instead of 6-311G(d,p) to compute the shielding constants changes the ^{13}C values of both TMS and corannulene very little (by 1.2 ppm or less).

The ^{13}C NMR chemical shifts were calculated with respect to the computed ^{13}C shielding constant in TMS, and the ^{7}Li NMR chemical shifts with respect to the computed ^{7}Li shielding constant in Li^+ (95.4 ppm). The nuclear independent chemical shifts[48] were computed as a negative of the shielding constant in the center of a ring (the mean of the carbon atom coordinates).

The notation used throughout the paper is as follows. The five innermost carbon atoms are denoted as hub carbons (C_h), and the 10 outermost as rim carbons (C_r).[49] The remaining five carbons, located at the "bridges" between the rim and hub of corannulene, are called "bridgehead rim" atoms (C_b) (Figure 1). We use the following notation for the protonated and lithiated corannulene isomers with H or Li on the external (convex) side of the corannulene bowl: σ_h, σ_b, and σ_r are complexes with attachment of H to one C_h, C_b, or C_r atom; η^2_{hh}, η^2_{hb}, η^2_{br}, and η^2_{rr} are bridged complexes with H or Li attached to two carbons; π_5 and π_6 are π-face complexes (the subscript number shows the number of carbons in the ring). For isomers with H or Li on the internal (concave) side of the bowl, a subscript "i" will be added, e.g. π_{5i} and π_{6i}.

3. Results and Discussion

3.1. Protonation of Corannulene. A corannulene molecule has several potential sites for protonation. The proton can bind to one carbon atom, attach to a C−C bond, or position itself over a ring, giving a σ-complex, a bridged complex, or a π-face complex, respectively. We considered all the above-mentioned possibilities and found that σ-complexes are the most favorable and that π-face complexes are the least favorable arrangements (Table 1). Structural and energetic features of the computed complexes are considered in more detail below.

Three convex σ-protonated corannulene isomers were located and proven to be at local minima. The σ_h isomer (Figure 2) was found to have the best total energy, with the σ_r isomer being only slightly (1.8 kcal mol^{-1}) higher, and the σ_b isomer being considerably (13.7 kcal mol^{-1}) higher. An attempt was made to find σ_{hi} and σ_{bi} complexes with hydrogen attached to the concave side of corannulene; however, these structures undergo bowl-to-bowl inversion with no activation barrier, leading to the convex protonated isomers. For σ_r, the convex and concave forms are identical, unless isotopomers are involved.

The relative energies of the three σ-complexes can be rationalized with the help of the π-orbital axis vector (POAV)

Table 1. Protonated Corannulene Isomers: Distances from the Attached Proton to the Nearest Carbon(s) (C−H^+) in Å, Proton Affinities (PA), and Enthalpies Relative to the Most Stable Isomer (Hrel) at 298 K (both in kcal mol^{-1}), as Computed at B3LYP/6-311G(d,p)

structure	C−H^+	PA	H_{rel}
σ_h	1.109	208.4	0
σ_r	1.106 (convex) 1.099 (concave)	206.6	1.8
σ_b	1.120	194.7	13.7
η^2_{hh} (TS σ_h−σ_h)	1.316	186.8	21.6
η^2_{hb} (TS σ_h−σ_b)	1.404 (C_h), 1.264 (C_b)	185.2	23.2
η^2_{br} (TS σ_b−σ_r)	1.289 (C_b), 1.349 (C_r)	182.5	25.9
η^2_{rr} (TS σ_b−σ_r)	1.328	190.1	18.3
π_5	1.629	142.9	65.5
π_{5i}	1.535	152.6	55.8
TS for bowl-to-bowl inversion in σ_r	1.102	198.2	10.2

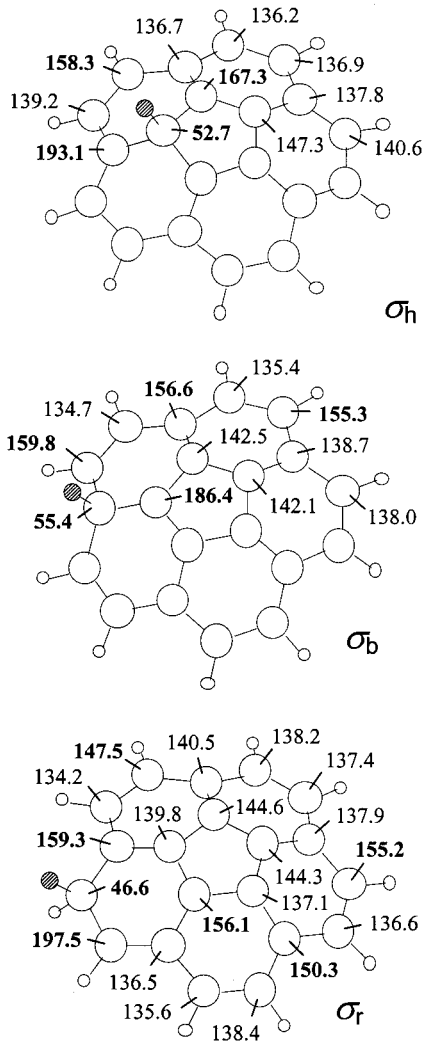

Figure 2. σ-Protonated corannulene isomers and ^{13}C NMR chemical shifts (in ppm). Proton attached to the hub (σ_h), bridgehead rim (σ_b), and rim (σ_r) carbons, respectively. Large open circles, carbons; small open circles, hydrogens; small dashed circle, attached hydrogen. Chemical shifts that differ by more than 10 ppm from the values in corannulene (140.4, 136.0, and 133.1 ppm for the hub, bridgehead rim, and rim carbons, respectively) are given in bold.

(47) Jameson, A. K.; Jameson, C. J. *Chem. Phys. Lett.* **1987**, *134*, 461.
(48) Schleyer, P. v. R.; Maerker, C.; Dransfeld, A.; Jiao, H.; Hommes, N. J. R. v. E. *J. Am. Chem. Soc.* **1996**, *118*, 6317.
(49) Rabideau, P. W.; Marcinow, Z.; Sygula, R.; Sygula, A. *Tetrahedron Lett.* **1993**, *34*, 6351.

Table 2. Pyramidalization Angles (θ, deg) for the Protonated Carbon in σ_h, σ_r, and σ_b

carbon	θ in corannulene	θ in Cor-H$^+$
C_h	8.3	18.0
C_b	3.8	12.8
C_r	1.6	16.8

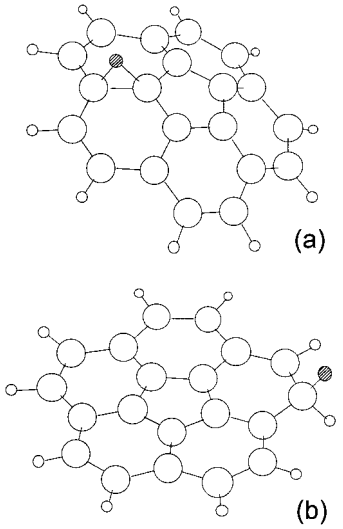

Figure 3. (a) Transition state between the σ_h and σ_b complexes, η^2_{hb}. (b) Transition state for the bowl-to-bowl inversion in the σ_r complex. Large open circles, carbons; small open circles, hydrogens; small dashed circle, attached hydrogen.

analysis.[50] POAV is defined as "that vector which makes equal angles ($\theta_{\sigma\pi}$) to the three σ-bonds at a conjugated carbon atom, and the pyramidalization angle is obtained as $\theta_P = (\theta_{\sigma\pi} - 90°)$.[50] The computed pyramidalization angles for the protonated carbons in σ_h, σ_b, and σ_r are given in Table 2. Pyramidalization angles in the low-energy protonated complexes σ_h and σ_r (18.0° and 16.8°) are within 3° from the ideal value (19.47°) for the sp^3-hybridized carbon. Every hub carbon atom is already pyramidalized in the parent corannulene ($\theta_P = 8.3°$), and this apparently facilitates attachment of a proton. A rim carbon has only a small pyramidalization in the parent corannulene ($\theta_P = 1.6°$), but this carbon is attached to a hydrogen that can easily be bent further out of plane when a second hydrogen is attached.

In contrast, the pyramidalization angle in σ_b (12.8°) is 6.7° smaller than the ideal tetrahedral angle. The bridgehead rim carbon has only a small pyramidalization in the parent corannulene ($\theta_P = 3.8°$), and the rigidity of the carbon skeleton hinders pyramidalization of this carbon upon protonation. The σ_b complex is higher in energy than σ_h and σ_r due to the steric strain. The bond between the carbon and the attached hydrogen in σ_b is longer than that in σ_h and σ_r (1.120 vs 1.109 and 1.106 Å, respectively), and has a lower ratio of the contributions of the carbon s to p orbitals (0.17 vs 0.21 in σ_h and 0.25 in σ_r, according to the NBO analysis).

The H-bridged isomers of protonated corannulene (an example is given in Figure 3a) are at first-order saddle points, and are transition states between the σ-complexes, as was proven with the IRC method. The C−H distances in these isomers are in the range 1.26−1.40 Å, i.e., longer by 0.15−0.30 Å than in σ-complexes. The activation enthalpies for isomerization of the σ-complexes can be obtained as differences between enthalpies

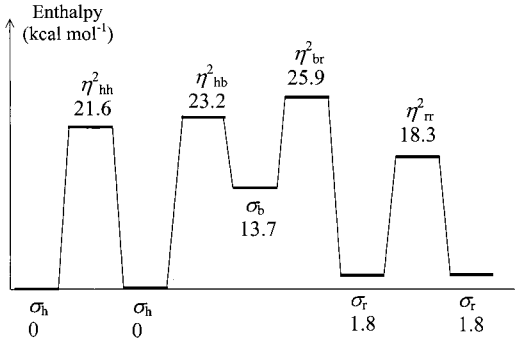

Figure 4. Enthalpy diagram of the σ and η^2 protonated corannulene isomers.

of σ-complexes and H-bridged complexes. Isomerization of the least favorable σ_b is predictably easiest (barriers are 9.5 kcal mol^{-1} for forming C_h−H and 12.2 kcal mol^{-1} for forming C_r−H). Isomerization of the σ_h or σ_r complexes requires a higher activation energy. Starting from the σ_h complex, one finds that the degenerate σ_h−σ_h shift has the lowest barrier (21.6 kcal mol^{-1}), followed by σ_h−σ_b (23.2 kcal mol^{-1}), and finally by σ_b−σ_r (25.9 kcal mol^{-1} with respect to σ_h, Figure 4). Starting from the σ_r complex, one finds the following sequence: σ_r−σ_r shift has the lowest barrier (16.5 kcal mol^{-1}), then σ_r−σ_b (24.1 kcal mol^{-1}), and finally σ_b−σ_h (21.4 kcal mol^{-1} with respect to σ_r) that allows formation of the equilibrated amount of the σ_h complex.

In addition to σ-complexes and H-bridged complexes, π-face complexes with the proton located on the C_5 symmetry axis were computed. The C−H distances in π_5 and π_{5i} are 1.629 and 1.535 Å, respectively. These structures are at 2nd order stationary points, and are much higher in energy (π_5 by 65.5 kcal mol^{-1}, and π_{5i} by 55.8 kcal mol^{-1}) than the σ_h complex. No stationary points were found corresponding to the π-face protonation of a six-membered ring.

It is interesting to see how protonation affects the barrier for bowl-to-bowl inversion in corannulene. Seiders et al.[51] have recently analyzed the inversion barriers in a number of substituted corannulenes. They have shown that bulky substituents placed in the *peri* positions cause a flattening of the corannulene bowl and a decrease of the barrier. Conversely, annelation across the *peri* positions causes a deepening of the bowl and an increase of the barrier.

The barrier in the parent corannulene, computed at B3LYP/6-311G(d,p), is 9.6 kcal mol^{-1}.[9] For the rim-protonated corannulene, our calculations predict the barrier of 8.4 kcal mol^{-1}, i.e., close to that in the parent molecule. The transition state (Figure 3b) has all atoms, with the exception of the two hydrogens bound to the same carbon, located in one plane. For the hub and bridgehead rim protonated corannulenes, there are no stable products of the bowl-to-bowl inversion. To estimate the energy required for flipping these isomers, we attached a proton to C_h or C_b from inside the corannulene bowl, and optimized positions of this proton and the protonated carbon while fixing all other atoms at positions they occupy in the parent corannulene. The estimates obtained are ca. 36 kcal mol^{-1} for σ_h and ca. 20 kcal mol^{-1} for σ_b, i.e., protonation of corannulene at C_h or C_b strongly hinders the bowl flipping.

Now we discuss the proton affinity of corannulene. The B3LYP/6-311G(d,p) values are 208.4, 206.6, and 194.7 kcal mol^{-1} for formation of the C_h−H, C_r−H, and C_b−H complexes, respectively. To estimate the precision of the computational

(50) (a) Haddon, R. C.; Scott, L. T. *Pure Appl. Chem.* **1986**, *58*, 137. (b) Haddon, R. C. *J. Am. Chem. Soc.* **1986**, *108*, 2837.

(51) Seiders, J. T.; Baldridge, K. K.; Grube, G. H.; Siegel, J. S. *J. Am. Chem. Soc.* **2001**, *123*, 517.

Table 3. Computed at B3YP/6-311G(d,p) and Experimental Proton Affinities (PA) of Benzene, Naphthalene, and Azulene, in kcal mol^{-1}

base	PA, expt.	PA, computed	deviation
benzene	179.9	184.2	+ 4.3
naphthalene	191.7	198.2	+ 6.5
azulene	221.1	225.9	+ 4.8

Table 4. Extrapolated Proton Affinities (PA) and Gas-Phase Basicities (GB) for Protonation of Corannulene at C_h, C_b, and C_r (both in kcal mol^{-1}), at $T = 298$ K

protonation at	PA, computed	PA, extrapolated	$T\Delta S$	GB
C_h	208.4	203.2	6.5	196.7
C_b	194.7	189.5	6.1	183.4
C_r	206.6	201.4	6.3	195.1

method employed, we calculated the experimentally measured proton affinities of benzene, naphthalene, and azulene using the same procedure. Comparison of the computed with experimental[52] proton affinities (Table 3) indicates that the computed values are consistently overestimated by 4−6 kcal mol^{-1} (on average 5.2 kcal mol^{-1}). This allows us to extrapolate corrected values (Table 4) for protonation of corannulene to be 203.2, 201.4, and 189.5 for formation of the C_h−H, C_r−H, and C_b−H complexes, respectively. Table 4 also contains the computed gas-phase basicities for corannulene {GB = PA − 298 K × ΔS(298K)}. The ΔS terms have been obtained from the Gaussian 98 frequency calculations.

Since the corannulene carbon skeleton resembles a fragment of the C_{60} fullerene surface, their protonated forms may be expected to be structurally similar. One can speculate that binding of the proton to one carbon of C_{60} should be preferred over bridged or π-face binding. Furthermore, the proton affinity of C_{60} should be close to that of a hub carbon in corannulene, as this is the most similar by pyramidality and surroundings to the C_{60} carbons. The larger π-system of C_{60}, facilitating accommodation of the positive charge, may result in a higher proton affinity than that of corannulene. On the other hand, the presence of 20 electropositive hydrogen atoms in corannulene may lead to the opposite result. The gas-phase basicity of 197.8 kcal mol^{-1} for C_{60} has been experimentally measured.[53] The computed gas-phase basicity of corannulene at the hub carbon is 196.7 kcal mol^{-1} (Table 4), which is very close to the experimental GB of C_{60}. This indicates that the effects of π-system size and of the presence/absence of peripheral hydrogens are either small or almost cancel each other.

3.2. Coordination of Corannulene to the Lithium Cations. As in the case of protonation described above, different modes of binding of the Li$^+$ cation to corannulene were explored. We found geometries of the π-face and bridged complexes. For the sake of completeness, we also performed a search of the complexes with attachment of Li$^+$ to one carbon only (analogous to the σ_h, σ_r, and σ_h protonated complexes), and found that no such complexes with Li$^+$ are at a stationary point. π-Face complexes of the lithium cation with corannulene are the most favorable, in contrast to the complexes with the proton.

Four π-face isomers were located (Figure 5); 6-convex, 5-convex, 6-concave, and 5-concave all are at local minima. The C−Li distances vary over the range 2.25−2.44 Å. The data in Table 5 indicate that the 6-convex complex is at the global minimum, the 5-convex is higher in energy by 0.2 kcal mol^{-1},

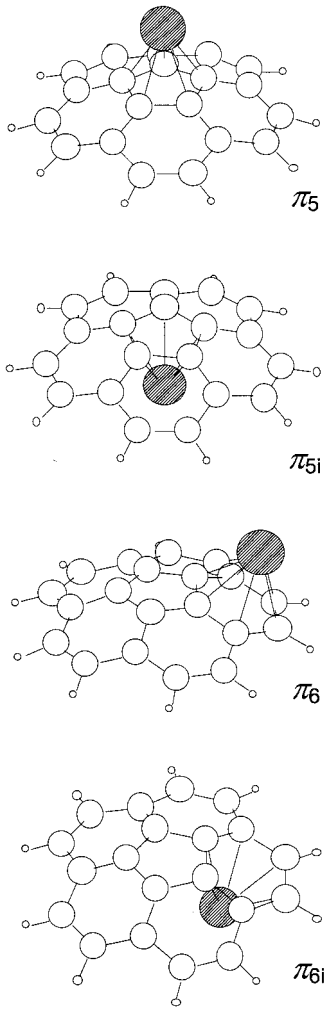

Figure 5. π-Face complexes of corannulene with the lithium cation: convex 5-ring (π_5), concave 5-ring (π_{5i}), convex 6-ring (π_6), and concave 6-ring (π_{6i}). Large open circles, carbons; small open circles, hydrogens; large dashed circle, lithium.

the 6-concave is higher in eneryg by 3.0 kcal mol^{-1}, and the 5-concave is higher in energy by 5.1 kcal mol^{-1}. Thus, convex complexes are lower in energy than concave complexes, the 6-convex complex is favored over the 5-convex complex, and the 6-concave complex is favored over the 5-concave complex. The difference between the 6-ring and 5-ring complexes is probably due to the larger number of carbon atoms in the "first coordination sphere" of the Li$^+$ cation in the former case. The lower energy of the convex complexes with respect to the concave complexes may be due to the electrostatic effects. Indeed, the dipole moment of corannulene (computed in this study to be 2.13 D) is directed along the C_5 axis, and its negative end is at the convex side of the bowl.

Three stationary points were found corresponding to the bridged complexes of Li$^+$ with corannulene (η^2_{hh}, η^2_{hb}, η^2_{hhi}) (two of them are shown in Figure 6). All three complexes possess one imaginary frequency. Complexes η^2_{hh} and η^2_{hb} are transition states for the Li$^+$ migration over the convex side of corannulene. The η^2_{hh} connects the 5-convex and 6-convex complexes, while the η^2_{hb} connects two equivalent 6-convex complexes. Activation energies for migrations over the convex side are small (5−6 kcal mol^{-1}). η^2_{hhi} connects concave complexes π_{5i} and π_{6i}, with even smaller activation energies (2.2 kcal mol^{-1} from π_{6i}, and only 0.1 kcal mol^{-1} from π_{5i}). No transition state connecting two π_{6i} complexes was located;

(52) Hunter, E. P. L.; Lias, S. G. *J. Phys. Chem. Ref. Data* **1998**, *27*, 413.

(53) McElvany, S. W.; Callahan, J. H. *J. Phys. Chem.* **1991**, *95*, 6186.

Table 5. Complexes of Corannulene with the Li^+ Cation: Distances from Li to the nearest Carbons or Hydrogens (C−Li or H−Li) in Å, Complex Formation Energies (ΔH_{Compl}), and Enthalpies Relative to the Most Stable Isomer (H_{rel}) (both in kcal mol^{-1}), as Computed at B3LYP/6-311G(d,p)//B3LYP/6-31G(d,p)

structure	C−Li or H−Li	ΔH_{compl} uncorrected for BSSE	ΔH_{compl} corrected for BSSE	H_{rel}
π_5	2.280	−44.9	−43.9	0.2
π_{5i}	2.254	−40.9	−39.0	5.1
π_6	2.293−2.443	−45.2	−44.1	0
π_{6i}	2.284−2.310	−42.6	−41.1	3.0
η^2_{hh} (TS π_5−π_6)	2.186	−40.4	−39.4	4.7
η^2_{hb} (TS π_6−π_6)	2.193, 2.209	−39.3	−38.3	5.8
η^2_{hhi} (TS π_{5i}−π_{6i})	2.176	−40.7	−38.9	5.2
TS for migration of Li across the edge (a)	1.799 (H−Li)	−20.0	−19.5	24.6
TS for migration of Li across the edge (b)	1.782 (H−Li)	−20.7	−20.1	24.0
TS for bowl-to-bowl inversion π_5 to π_{5i}	2.254	−33.0	−31.7	12.4
TS for bowl-to-bowl inversion π_6 to π_{6i}	2.286−2.385	−35.0	−33.8	10.3

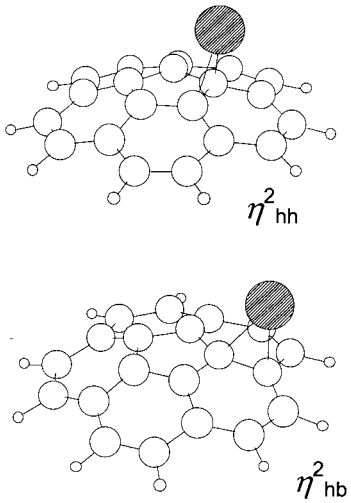

Figure 6. Transition states for the lithium cation migration over the convex side of corannulene: η^2_{hh} (between the π_5 and π_6 complexes) and η^2_{hb} (between two equivalent π_6 complexes). Large open circles, carbons; small open circles, hydrogens; large dashed circle, lithium.

attempts to find it led to the π_{5i} complex. Thus, a migration from one π_{6i} position to another is likely to proceed via the π_{5i} complex.

Migration of the Li^+ cation across the edge of corannulene, in contrast to the shifts along one side, involves a high barrier. Figure 7a,b shows complexes with Li^+ coordinated to two hydrogens of corannulene. Energies of these complexes are −20.1 and −19.5 kcal mol^{-1} with respect to the isolated Li^+ and corannulene, i.e., the binding of Li^+ is ca. 2.2 times weaker than that in the face π-complexes. Both complexes are at 1st-order saddle points, and the imaginary frequency in each complex corresponds to movement of the lithium atom from one side of corannulene to another. Because of the very long path to be traveled by Li^+ to reach a π-face position, we did not obtain the associated reactants and products by the IRC method. However, it is reasonable to assume that complexes π_6 and π_{6i} should be involved in the path for Li^+ migration between the corannulene sides. The barrier for such a migration is at least 24 kcal mol^{-1} starting from π_6, and 21 kcal mol^{-1} from π_{6i}.

An alternative process that will transform a convex complex to a concave complex is bowl-to-bowl inversion in the lithiated corannulene (transition states are shown in Figure 7c,d). The presence of the Li^+ cation makes the initial and the final states of bow-to-bowl inversion nonequivalent. The inversion barriers for the lower energy convex complexes are slightly higher (12.2 kcal mol^{-1} for π_5 and 10.3 kcal mol^{-1} for π_6) and for the higher energy concave complexes are slightly lower (7.3 kcal mol^{-1} for both π_{5i} and π_{6i}) than that for free corannulene (9.6 kcal mol^{-1}). The average barrier height, 9.8 kcal mol^{-1} for 5-ring and 8.8 kcal mol^{-1} for 6-ring complexes, appears almost unaffected by the attachment of Li^+. Note that a transformation between the convex and concave complexes via bowl-to-bowl inversion has a much lower barrier than the Li^+ migration across the corannulene edge.

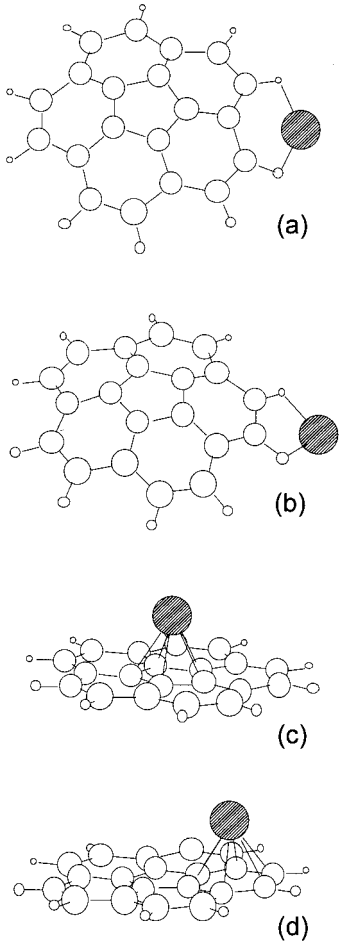

Figure 7. Transition states: (a, b) migration of the lithium cation across the edge of corannulene; (c) bowl-to-bowl inversion in the π_5 complex; (d) bowl-to-bowl inversion in the π_5 complex. Large open circles, carbons; small open circles, hydrogens; large dashed circle, lithium.

3.3. NMR Shielding Constants and Chemical Shifts. To further explore the electronic properties of protonated coran-

nulene isomers and complexes of corannulene with the lithium cation, we performed calculations of the NMR chemical shifts. The chemical shift (δ) is defined as

$$\delta = \sigma_{ref} - \sigma$$

where σ and σ_{ref} are the NMR shielding constants of a given atom in the compound under study and in a reference compound, respectively. For the ^{13}C chemical shifts, tetramethylsilane (TMS) is typically used as a reference. Note that the chemical shift is positive when the shielding constant in the compound under study is lower than that in the reference compound.

The NMR chemical shifts, either experimentally measured or computed, are a valuable source of information on the electronic structure.[54] The chemical shift often depends on the electron density on a given atom, a lower density usually causing a higher shift. Unsaturated rings in the neighborhood of a given atom also influence the NMR chemical shift.[48,55,56] Aromatic rings possess diatropic ring currents and cause negative shifts, whereas antiaromatic rings with paratropic currents cause positive shifts.

3.3.1. ^{13}C Chemical Shifts in Protonated and Neutral Corannulene. The computed ^{13}C chemical shifts of neutral corannulene are 140.4, 136.0, and 133.1 ppm for the hub, bridgehead rim, and rim carbon atoms, respectively. These values are close to the experimental measurements by Orendt et al.[57] (135, 130, and 127 ppm at 298 K). The computed shifts correlate with the computed natural charges on the carbon atoms of each type (hub, −0.01 e; bridgehead rim, −0.05 e; rim, −0.17 e; carbons in tetramethylsilane, −1.06 e). A possible explanation is that the rim carbons of corannulene have the smallest shifts because they are each bound to a hydrogen atom and pull some electron density from that atom; by comparison, the hub carbons have the largest shifts because they are the furthest removed from hydrogen atoms.

Protonation of corannulene strongly (by more than 80 ppm) decreases the chemical shift on the carbon atom that accepts the hydrogen (the computed ^{13}C shifts are 52.7, 55.4, and 46.6 ppm for the σ_h, σ_b, and σ_r complexes, respectively). This is in line with the increased electron density on that carbon (natural charges are −0.32 e in σ_h, −0.36 e in σ_b, and −0.48 e in σ_r), due to the formation of a covalent σ bond with the newly attached hydrogen. On the other hand, increased chemical shifts are observed on all carbons other than the protonated one. Particularly notable are the greatly increased (by 16−54 ppm) shifts on the carbons located in the ortho and para positions with respect to the protonation site in the six-membered rings (see Figure 2). In the σ_h complex, for instance, the shift on the hub carbons neighboring the protonated carbon (ortho position) is 167.3 ppm, on the bridgehead rim carbon (other ortho position) −193.1 ppm, and on the rim carbons in the para position −158.3 ppm.

3.3.2. Probing the Aromaticity of the Protonated and Neutral Corannulene with Nuclear-Independent Chemical Shifts (NICS). The magnetic ring currents in the compounds containing aromatic or antiaromatic rings have been shown to strongly influence the NMR chemical shifts on the adjacent atoms located near the ring axis, e.g. on coordinated lithium cations[55,58−60] and on ^{3}He atoms encapsulated in C_{60}.[61] Schleyer et al.[48] proposed the use of nuclear independent chemical shift (NICS) as a probe of ring aromaticity. The NICS value is the negative of the shielding constant in the center of a ring (in some cases, shielding constants at a point 1 Å above the plane of the ring are more informative[62]).

Before discussing the influence of protonation on the aromaticity of corannulene rings, we have to consider the NICS in neutral corannulene. To our knowledge, aromaticity of the individual rings in corannulene has not previously been investigated. Pasquarello et al. studied ring currents in fullerenes C_{60},[63,64] C_{70},[64] and their hexaanions.[64] They concluded that the six-membered rings of C_{60} and C_{70} are aromatic (possess diatropic currents), whereas the five-membered rings are antiaromatic (possess paratropic currents). This prediction received an experimental confirmation in the NMR study of substituted C_{60}.[56] For acenaphthylene and pyracyclene, two smaller polycyclic hydrocarbons, the same pattern of aromatic six-membered rings neighboring antiaromatic five-membered rings was predicted in the NICS calculations.[48]

Our NICS calculations for the neutral corannulene yielded values +8.1 ppm for the five-membered ring and −7.0 ppm for the six-membered rings. These values indicate the antiaromatic character of the former and aromatic character of the latter, i.e., corannulene fits the pattern of the C_{60} and C_{70} fullerenes, acenaphthylene, and pyracyclene. For the complexes of corannulene with metals, the computed NICS values suggest that the NMR chemical shift on the metal should be negative when it is coordinated to the six-membered ring, and positive when it is coordinated to the five-membered ring. Our calculations on the Li$^+$ complexes (see below) indicated that this is the case for convex complexes, but not for concave complexes.

Because of the nonplanarity of corannulene, a question arises whether the size of the "antiaromatic" region associated with the five-membered ring is different on the convex and the concave side. To address this issue, we computed the NICS along the C_5 axis of corannulene. The results presented in Figure 8 indicate that the "antiaromatic" area spreads to a much greater distance on the convex side of the bowl (ca. 1.7 Å vs ca. 0.8 Å on the concave side). For the metal complexes of corannulene, this suggests that the NMR chemical shift of atoms coordinated to the convex side should be significantly different from those on the concave side. This is indeed the case for the Li$^+$ complexes of corannulene discussed below.

Having considered the NICS in the neutral corannulene, we will now address changes of the ring aromaticity upon protonation. The computed NICS in the centers of rings of the protonated corannulene isomers are shown in Figure 9. In the σ_h complex, NICS for all rings are negative, indicating their aromatic character. It is particularly remarkable that the character of the five-membered ring changes from antiaromatic in

(54) Wilson, E. K. *Chem. Eng. News* **1998**, *Sept. 28*, 25.
(55) Paquette, L. A.; Bauer, W.; Sivik, M. R.; Buehl, M.; Feigel, M.; Schleyer, P. v. R. *J. Am. Chem. Soc.* **1990**, *112*, 8776.
(56) Prato, M.; Suzuki, T.; Wudl, F. *J. Am. Chem. Soc.* **1993**, *115*, 7876.
(57) Orendt, A. M.; Facelli, J. C.; Bai, S.; Rai, A.; Gossett, M.; Scott, L. T.; Boerio-Goates, J.; Pugmire, R. J.; Grant, D. M. *J. Phys. Chem. A* **2000**, *104*, 149.
(58) Jiao, H.; Schleyer, P. v. R. *Angew. Chem., Int. Ed. Engl.* **1993**, *32*, 1763.
(59) (a) Cox, R. H.; Terry, H. W., Jr. *J. Magn. Reson.* **1974**, *14*, 317. (b) Cox, R. H.; Terry, H. W., Jr.; Harrison, L. W. *J. Am. Chem. Soc.* **1971**, *93*, 3297.
(60) Exner, M. M.; Waack, R.; Steiner, E. C. *J. Am. Chem. Soc.* **1973**, *95*, 7009.
(61) Buehl, M.; Thiel, W.; Jiao, H.; Schleyer, P. v. R.; Saunders: M.; Anet, F. A. L. *J. Am. Chem. Soc.* **1994**, *116*, 6005.
(62) Schleyer, P. v. R.; Jiao, H.; Hommes, N. J. R. v. E.; Malkin, V. G.; Malkina, O. L. *J. Am. Chem. Soc.* **1994**, *116*, 6005.
(63) Pasquarello, A.; Schlueter, M.; Haddon, R. C. *Science* **1992**, *257*, 1660.
(64) Pasquarello, A.; Schlueter, M.; Haddon, R. C. *Phys. Rev. A* **1992**, *47*, 1783.

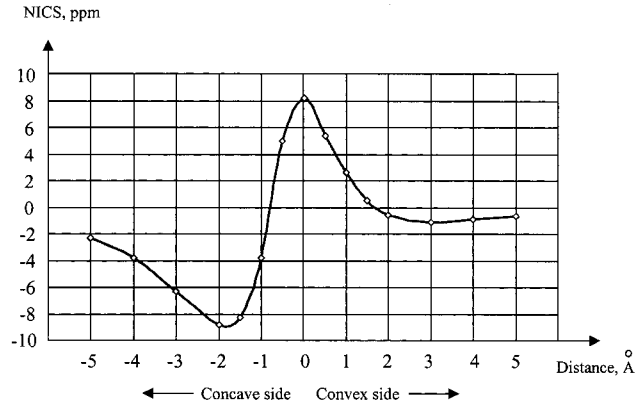

Figure 8. Plot of the NICS value (in ppm, axis *Y*) vs the distance from the plane of the five-membered ring of corannulene (in Å, axis *X*). Points are taken on the C_5 symmetry axis of corannulene.

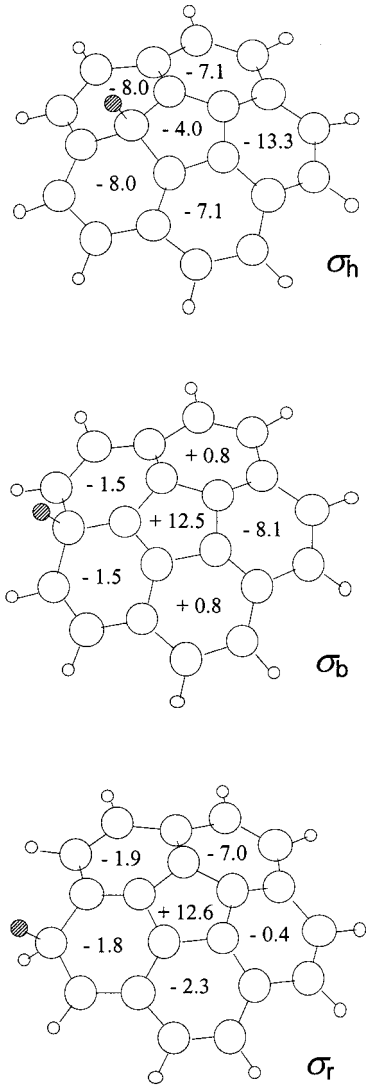

Figure 9. NICS values in the ring centers of tautomers of protonated corannulene (in ppm). For neutral corannulene NICS values are −7.0 ppm for the six-membered rings and +8.1 ppm for the five-membered ring.

corannulene to aromatic in the σ_h complex. The aromaticity of the six-membered rings somewhat increases when this complex is formed.

In the σ_b and σ_r complex, in contrast to σ_h, the NICS for the five-membered ring is positive and is larger than in corannulene, indicating an increase in the ring antiaromaticity. Aromaticity of the six-membered rings in these complexes is smaller than that in corannulene (an exception is one ring in σ_b whose NICS is somewhat more negative than that in corannulene). Two rings in σ_b even possess a positive NICS, i.e., are slightly antiaromatic.

Table 6. ^{7}Li NMR Chemical Shifts in the Complexes of Li^+ with Corannulene (in ppm)

complex	shift from the free Li^+, ppm
π_5	+1.3
π_{5i}	−9.6
π_6	−1.9
π_{6i}	−9.2

The average values of NICS for all rings are −7.9 for σ_h, +0.5 for σ_b, and −0.1 for σ_r, compared to −4.5 for corannulene. This indicates that the overall aromaticity of corannulene increases upon protonation at a hub carbon and decreases upon protonation at a rim or bridgehead rim carbon. The increased aromaticity of the σ_h complex is consistent with its better total energy with respect to σ_b. However, the σ_r complex, despite its low average aromaticity, is almost as low in energy as σ_h (see Section 3.1). This is probably due to the lower amount of steric strain involved in proton attachment to a rim carbon.

3.3.3. ^{7}Li Chemical Shifts in the Complexes of Corannulene with the Li^+ Cation. The NMR chemical shift (experimentally measured or computed) of a Li cation coordinated to an organic ring can be used as a probe of ring aromaticity.[55,58,61] In the absence of ring current phenomena, the range of Li chemical shifts is restricted to ca. −2 to +2 ppm for most of organolithium compounds.[55] In contrast, a ^{7}Li chemical shift several times larger in magnitude is observed when Li^+ is coordinated to an aromatic ring, e.g. −8.37 ppm in cyclopentadienyllithium,[59] −13.3 ppm in (9-(2-hexyl)fluorenyl)lithium,[60] and ca. −15 ppm predicted by calculations for $Li^+@C_{60}$.[61]

The computed ^{7}Li NMR chemical shifts in the Li^+ complexes with corannulene are listed in Table 6. Negative and remarkably large shifts are predicted for the concave complexes: −9.2 ppm for π_{6i} and −9.6 ppm for π_{5i}. The negative sign of the ^{7}Li shift in π_{6i} is in line with the aromatic character of the six-membered ring (NICS = − 7.0 ppm). The ^{7}Li shift in π_{5i} is negative despite the antiaromatic character of the five-membered ring (NICS = + 8.1 ppm). This is likely due to the short span of the "antiaromatic" region on the concave side of the five-membered ring. This region extends only to ca. 0.8 Å from the ring plane (see Figure 9). The Li^+ cation in π_{5i} is located at ca. 1.9 Å from the ring plane, and the NICS value for that point is negative (ca. − 8.9 ppm).

In the convex π_5 complex, the computed shift is positive (+1.3 ppm), in line with the antiaromaticity of the five-membered ring. The "antiaromatic" region on the convex side of the ring extends to ca. 1.7 Å from the ring plane in corannulene (Figure 9), and probably somewhat further in the complex with Li^+, so that Li^+ at ca. 1.9 Å is under antiaromatic influence.

In the convex π_6 complex, the predicted ^{7}Li shift (−1.9 ppm) is negative, but is much smaller than that in π_{6i}. This may be a sign that the shift in the concave π_{6i} complex is due to the influence of not only the ring to which Li^+ is coordinated, but also the four other six-membered rings. Because of the bowl shape of corannulene, the influence of noncoordinated six-membered rings should be smaller in the π_6 complex than in the π_{6i} complex.

4. Conclusion

A computational modeling of the binding of protons and lithium cations to corannulene has been performed. All three σ-protonated isomers are found to be at local minima on the potential energy surface. The isomer protonated at the innermost (hub) carbon has the best total energy. Protonation at the outermost (rim) carbon is slightly (ca. 2 kcal mol^{-1}) less favorable, and protonation at the intermediate (bridgehead rim) carbon is significantly (ca. 14 kcal mol^{-1}) less favorable than that at the hub carbon. Hydrogen-bridged isomers are transition states between the σ-complexes. The activation energies required to transform one σ-complex to another vary from 10 to 26 kcal mol^{-1}. The best estimate for proton affinity of corannulene is 203 kcal mol^{-1}.

Complexes of Li^+ with corannulene at local minima are those with π-face binding of the cation. There is a small energetic preference for the 6-ring over the 5-ring binding (up to 2 kcal mol^{-1}) and of the convex face over the concave face binding (3−5 kcal mol^{-1}). The Li-bridged complexes are transition states between the π-face complexes. Movement of the Li^+ cation over either face is facile, and the activation energy does not exceed 6 kcal mol^{-1} on the convex face and 2.2 kcal mol^{-1} on the concave face. In contrast, transition of Li^+ across the corannulene edge involves a high activation barrier (24 kcal mol^{-1} with respect to the lowest energy π-face complex). An easier way for the transformation of the concave complexes to convex and vice versa is the bowl-to-bowl inversion, with an activation energy of 7 to 12 kcal mol^{-1}. The computed binding energy of Li^+ to corannulene is 44 kcal mol^{-1}.

Aromaticity of the rings of corannulene and its changes upon protonation have been analyzed by means of computing the ^7Li NMR chemical shifts and nuclear independent chemical shifts (NICS). In the neutral corannulene, the central five-membered ring is antiaromatic, whereas the peripheral six-membered rings are aromatic. The antiaromatic area stretches to a larger distance on the convex side of the corannulene bowl than on the concave side. Due to that, a lithium cation in the convex π_5 complex experiences an antiaromatic influence (the ^7Li NMR chemical shift is positive), while a lithium cation in the concave π_{5i} complex experiences an aromatic influence (the shift is negative). Protonation of corannulene at a hub carbon, according to the NICS analysis, makes the central ring aromatic, and enhances aromaticity of the peripheral rings. In contrast, protonation at a rim carbon or a bridgehead rim carbon enhances antiaromaticity of the central ring, and reduces the average aromaticity of the peripheral rings.

Acknowledgment. The authors thank Professor Lawrence Scott for helpful information and the Natural Science and Engineering Research Council of Canada for the financial support of this research.

Supporting Information Available: Tables of experimental data (PDF). This material is available free of charge via the Internet at http://pubs.acs.org.

JA0021464